

Design Study of Friction Nanogenerator Based on Bionic Electric eel Structure

Zhirao Yin, Shaojun Zhang*, Rui Sun, Chun Zhao, Qianyong Zhang

School of Shandong Jiaotong University, Weihai 510000, China

*Corresponding author

Abstract

There exists a large amount of multidirectional and low-frequency wave energy in the ocean, and the emerging friction nanogenerator is quite advantageous in collecting the multidirectional and low-frequency wave energy in the ocean and converting it into electrical energy compared with the traditional ocean energy harvesting devices. Inspired by the biological structure of electric eel, a friction nanogenerator (BE-TENG) modeled after the electric eel is designed as a novel energy-loading device in this paper. In this paper, we firstly designed the BE-TENG structure with a semi-cylindrical shell as the main body, combined with a crankshaft-like structure and a biomimetic fin swing rod to simulate the electric eel's tail fins to ensure the balance of the device; secondly, we proposed a helical power generation structure, and the short-circuit current under the same conditions increased from 1.37 μA to 3.05 μA compared with the ordinary PTFE-Al friction pair, which is a 2.23-fold enhancement; and thirdly, this paper explores the potential relationship between the BE-TENG dielectric layer and the electrode layer and the factors affecting the output performance of BE-TENG, and investigates the effective friction area between the composite dielectric layer and the electrode layer, the thickness of the composite dielectric layer, and the influence on the output performance of BE-TENG by controlling the single-factor variables; finally, under the conditions of the present experiments, it was obtained that the Finally, under the present experimental conditions, the best output performance of BE-TENG is obtained when the effective contact area between the BE-TENG composite dielectric layer and the electrode layer is $32\pi \text{ cm}^2$ and the thickness of the composite dielectric layer is 0.3 mm, and the optimized BE-TENG further improves its ability to collect blue energy, with a view to providing a new idea for the application of friction nano-generators and the protection of the blue ocean environment.

Keywords

Friction Nanogenerator; Bionic Electric Eel; Blue Energy; Structural Design.

1. Introduction

Ocean waves are an important renewable and clean energy source due to their abundant reserves, good energy quality, high energy flow density, greenness, and renewability; however, the complexity of the marine environment leads to many challenges and uncertainties in collecting wave energy. Although some progress has been made in the development and utilization of wave energy, it lacks cost-effective collection technology and is rarely exploited [1]. Nowadays, wave energy is mainly collected by first absorbing wave energy from a large area, concentrating it into mechanical energy, and then generating electricity using electromagnetic generators. However, it has problems such as complicated structure, high cost, mismatch between working frequency and wave frequency, large volume, poor durability and

stability, etc. It cannot effectively collect wave energy and is difficult to promote and utilize it on a wide scale, which leads to slow progress in the field of wave energy generation[2].

The invention of friction nanogenerator (TENG) provides a new way to convert wave energy into electrical energy, and this power generation technology shows good application prospects in collecting irregular and low-frequency blue energy. Aiming at the wave itself, which is fickle, multi-directional, and moves irregularly, friction nanogenerators have obvious advantages over traditional electromagnetic generators. The use of friction nanogenerators to collect wave energy is considered to be a green and sustainable new energy pathway, which has significant research value for the sustainable development of energy and is expected to realize the dream of blue energy[3].

The electric eel is one of the very few organisms in nature that uses electrical discharges for hunting or defense. The body of the electric eel is elongated and cylindrical, and the streamlined body contour helps to reduce the resistance of seawater. The body usually includes dorsal ventral and caudal fins, which help the electric eel to maintain stability and maneuverability in the water; most of the electric eel's internal structure consists of biocells composed of muscle lamellae and cells, and the electric eel is capable of outputting a voltage of up to 600 V through the series connection of hundreds of the same biocells and the parallel connection of electric eels [4]. Inspired by the biological structure of electric eel, this paper designs a friction nanogenerator (BE-TENG) as a new type of energy loading and unloading device, which provides theoretical and technical support to promote the development of friction nanogenerator, and facilitates the breakthroughs and advances in its practical applications.

2. Experimental Methods

2.1. BE-TENG Friction Layer Material Selection

Under the same environmental conditions, the selection of the friction dielectric layer largely determines the output power of the TENG, the application environment and so on [5]. Therefore, the selection of the dielectric layer material is crucial before constructing the TENG structure. In 2002, DK Davie et al [6] ranked the friction electronegativity sequence of some common materials as shown in Fig. 1. According to the ranking of material electronegativity, in this paper, rate foil, which is easy to lose electrons and has a positive surface charge, is selected as the electrode layer of BE-TENG, and polytetrafluoroethylene (PTFE), which is easy to gain electrons and has a negative surface charge, is selected as the dielectric layer of BE-TENG.

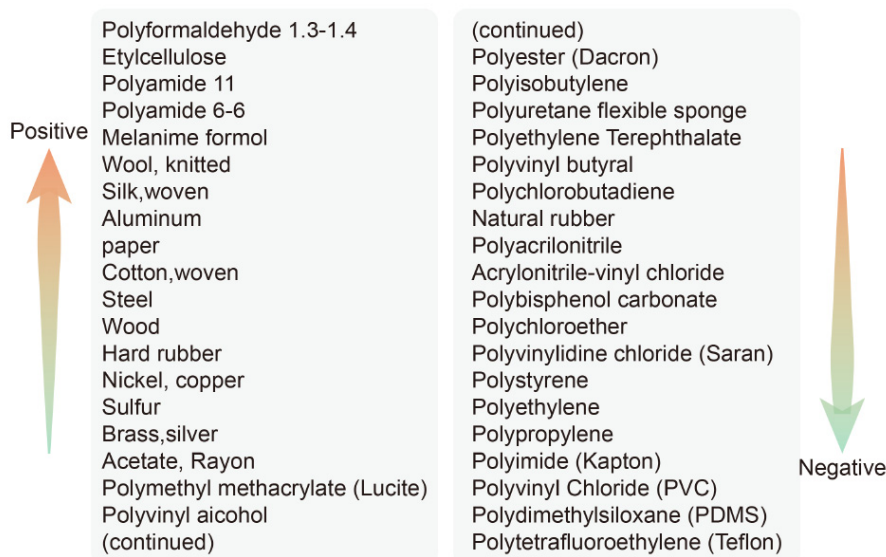


Fig 1. Electronegativity ranking of some common materials

2.2. Preparation of BE-TENG Electrode Layer

According to the aluminum foil located in the lower right of the friction electric sequence table in Fig. 1, it can be seen that the aluminum foil has a strong ability to lose electrons and is easily positively charged, while other metal materials such as copper foil do not have this characteristic compared to the aluminum foil, so the aluminum foil was used as the electrode layer material of the BE-TENG in this experiment.

Aluminum foil is cleaned by ultrasonic cleaning to remove surface impurities, dried at room temperature, repeatedly rolled by a roller machine until the surface is wrinkle-free, rinsed with anhydrous ethanol, and dried at room temperature to complete the preparation of the BE-TENG electrode layer material, and the preparation process of the BE-TENG metal electrode layer material is shown in Fig. 2.

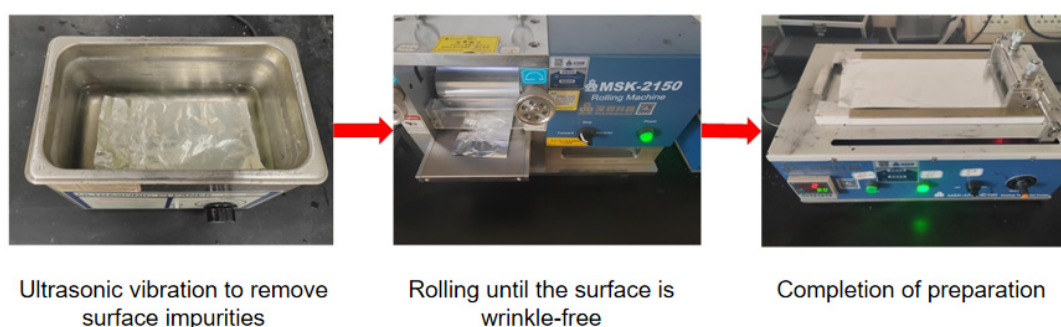


Fig 2. BE-TENG electrode layer material preparation process

2.3. Preparation of BE-TENG Dielectric Layer

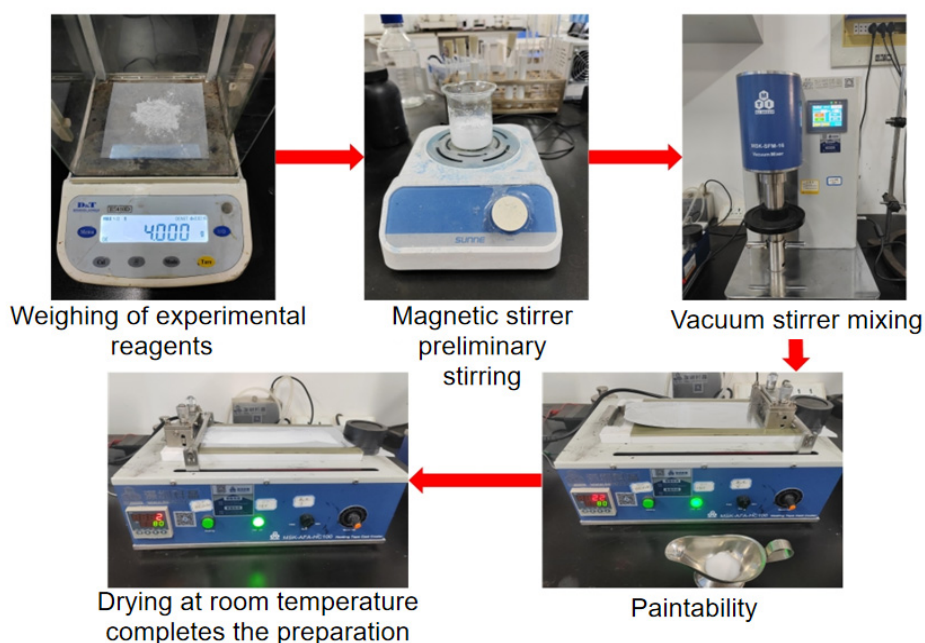


Fig 3. Preparation flow of PTFE dielectric layer for BE-TENG

Weigh polytetrafluoroethylene (PTFE) and adhesive to the beaker to dissolve, and placed in a magnetic stirrer stirring for 30 min, until the end of the stirring time, take out the mixture of PTFE and adhesive placed in a vacuum mixer, set the stirring time of 10 min, the speed of 600 r/min, and repeat the stirring until the mixture is uniformly blended and no fine particles. Take out the mixture of PTFE and adhesive and put it in a pipette, set the heating temperature of the

coater at 60°C and turn on the vacuum, place the made BE-TENG electrode layer flat on the coater, and put a scraper on the rightmost side of the BE-TENG electrode layer. After the temperature reaches the set temperature, use the dispensing dish to pour the mixture of PTFE and adhesive evenly in front of the squeegee, and start the coating machine to make the squeegee move forward at a uniform speed. When the squeegee moves to the leftmost side of the BE-TENG electrode layer to stop coating, make the squeegee reset and then repeat to start the coating machine until the mixture of PTFE and adhesive evenly covers the top of the BE-TENG electrode layer, and then dry it at room temperature to complete the preparation of the PTFE dielectric layer of the BE-TENG. The process of the preparation of the PTFE dielectric layer of the BE-TENG is shown in Fig. 3.

2.4. Structural Design of BE-TENG

The external structure of this device is derived from the biological structure of electric eel, and the external structure of the device is shown in Fig. 4. Considering that the application scenario of the BE-TENG device designed in this paper is on the sea surface, the humid environment is easy to affect the internal power generation structural materials and unnecessary material loss occurs, so the BE-TENG device adopts a closed structure to protect the internal materials; considering that the device is powered by the thrust of the sea waves, the device adopts a fully closed three-quarter cylindrical structure, the overall structure is a cylinder to simulate the electric eel's body shape. The bottom surface of the device is designed as a plane to increase the contact area between the bottom surface and the sea surface, so as to make the device better stressed; the bottom surface of the device is connected to the crankshaft structure, and several swinging lassos are connected to the crankshaft, which together simulate the anal fins and caudal fins connected to the electric eel, so as to ensure the device's balance in the sea, and it will not be overturned by the influence of the waves.

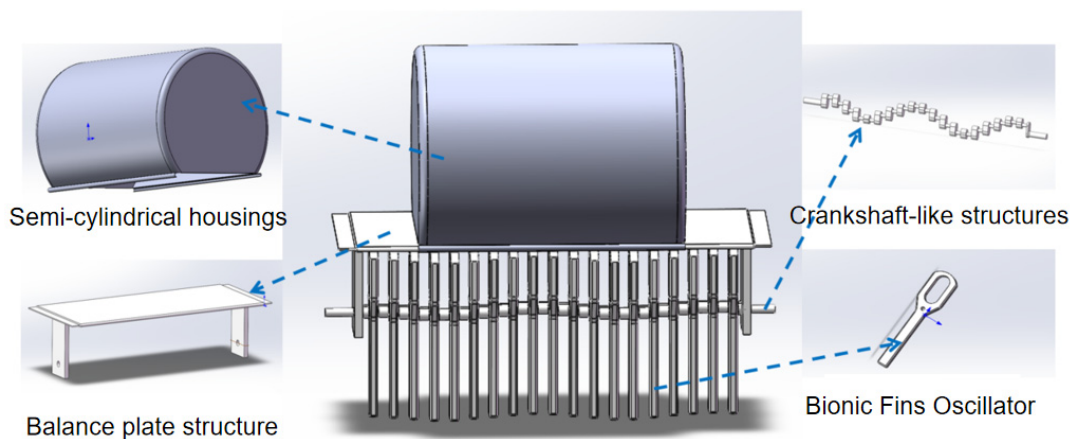


Fig 4. BE-TENG external structure

The internal structure design of this device is also derived from the power generation structure inside the body of an electric eel, and the internal structure of the device is shown in Fig. 5. The device proposed by Zou et al. in their paper can produce a peak voltage of 170 V under sometimes dry conditions, while sometimes there is no significant voltage output in relatively humid environments [], which shows that the water content in the power generation environment of the device affects the generator's efficiency of power production. However, the stretchable TENG designed by Zou's team is based on the solid-liquid contact mode, and the presence of liquid intervention leads to a humid working environment. Therefore, in this paper, we use the high-efficiency spiral structure proposed by Wei et al. to replace the power-

producing structure of the stretchable TENG [1]. The inner wall of the elastic spiral structure mimics the muscle sheet of an electric eel, and the collision between the conductive liquid and the silicone material is replaced by the collision of the inner wall of the spiral, which can reduce the humidity of the internal environment and increase the efficiency of the space utilization at the same time.

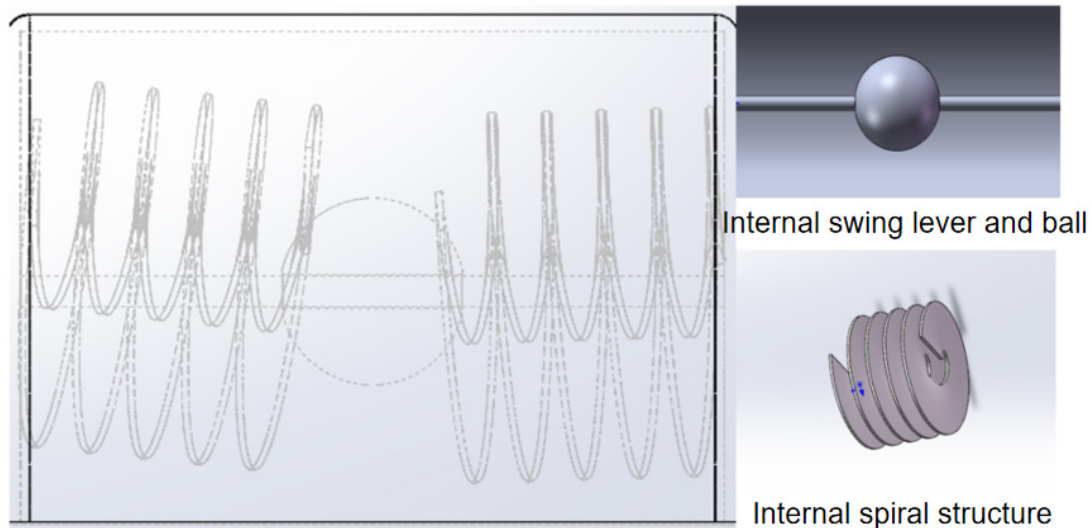


Fig 5. BE-TENG internal structure

After designing the structure of the BE-TENG device through SOLIDWORKS modeling software, the designed model was printed using a 3D printer. After printing, each part of the BE-TENG device was polished with sandpaper to remove surface burrs, so as to avoid the test failure due to the puncture of the electrode layer and dielectric layer by the surface burrs of the BE-TENG device parts. The polished BE-TENG parts are placed in the ultrasonic oscillator for ultrasonic cleaning to remove dust and other impurities on the surface of the parts, the cleaning time is set to 30 min, and after the cleaning time is over, the parts are rinsed with deionized water and air-dried.

3. Results and Discussion

3.1. Theoretical Modeling Analysis of BE-TENG Power Generation

BE-TENG is a device structure based on the vertical contact-separation mode of the four operating modes of friction nanogenerators. The friction nanogenerators in vertical contact-separation mode can be divided into: dielectric-dielectric materials and conductive-dielectric materials according to the material division. In this paper, the structure of conductive-dielectric (Al-PTFE) material is used for testing and design. As shown in Fig 6., the BE-TENG internal structure of the spiral structure body, the upper and lower surfaces were attached to PDMS, Al two materials constitute a nearly parallel plane, set the thickness of the PDMS friction layer is w_1 , Al friction layer thickness is w_2 , the relative permittivity of the PDMS is ϵ_1 , the relative permittivity of the Al is ϵ_2 . The surface of the PDMS and Al are attached a layer of copper foil metal electrodes, and let the distance between the friction pairs be $X(t)$, which changes under the action of external force. When the two friction layers are in contact with each other, due to the principle of electrostatic induction the surfaces of the two materials will take on an equal amount of dissimilar sign charge, set the density of the same charge on the two materials to be σ , ignoring the amount of loss of charge in a short period of time; when the two friction layers are separated from each other, an induced potential difference is generated through the copper foil electrodes, which is set to be V . In order to balance the potential difference, the electrons

move in the external circuit, and set the amount of induced charge transfer produced in this process to be $X(t)$. The amount of induced charge transfer produced is Q [7].

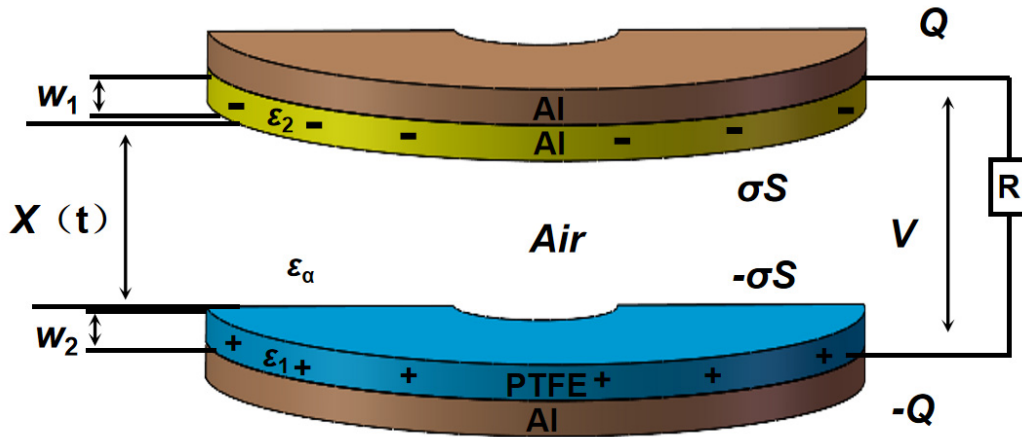


Fig 6. BE-TENG vertical contact theory model

According to Gauss's theorem, the electric field strength E_1 inside the PDMS material can be obtained as:

$$E_1 = -\frac{Q}{S\epsilon_0\epsilon_1} \quad (1)$$

The electric field strength E_2 inside the Al material is:

$$E_2 = -\frac{Q}{S\epsilon_0\epsilon_2} \quad (2)$$

The electric field strength E_{Air} of the air field between the friction pair is:

$$E_{Air} = -\frac{\frac{Q}{S} - \sigma(t)}{\epsilon_0} \quad (3)$$

The potential difference V between the friction pairs is:

$$V = E_1w_1 + E_2w_2 + E_{Air}X(t) \quad (4)$$

Associating the above equation, the potential difference V between PDMS and TENG with Al as the friction pair at a certain moment t is obtained as:

$$V = -\frac{Q}{S\epsilon_0} \left(\frac{w_1}{\epsilon_1} + \frac{X(t)}{\epsilon_\alpha} + \frac{w_2}{\epsilon_2} \right) + \frac{\sigma X(t)}{\epsilon_0\epsilon_\alpha} \quad (5)$$

In the process of BE-TENG device power production test, the external circuit is open-circuit state, at this time Q is 0, can be obtained at this time the open-circuit voltage (V_{oc}):

$$V_{oc} = \frac{\sigma X(t)}{\epsilon_0\epsilon_\alpha} \quad (6)$$

Meanwhile, when the external circuit of the BE-TENG device is in the short-circuit state, the voltage V between the electrodes is 0. Therefore, the transferred charge (Q_{sc}) and the short-circuit current (I_{sc}) in the short-circuit state can be obtained, respectively:

$$Q_{sc} = \frac{\sigma X(t)}{\epsilon_0w_0 + X(t)} \quad (7)$$

$$I_{SC} = \frac{dQ_{SC}}{dt} = \frac{S\sigma\varepsilon_0 w_0 v(t)}{(\varepsilon_0 w_0 + X(t))^2} \tag{8}$$

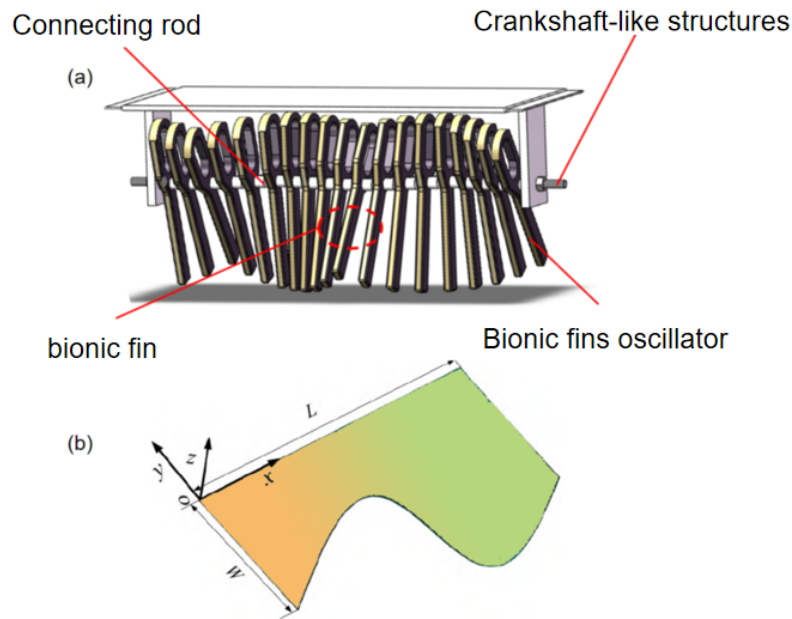
The capacitance C is obtained from the formula $C=V/Q$ for capacitance:

$$C = \frac{\varepsilon_0 S}{w_0 + X(t)} \tag{9}$$

In BE-TENG with PDMS and Al materials as friction pairs, electrons move back and forth between the copper foil electrodes to form an alternating current, at which point this power generator is equivalent to a capacitor, with displacement current in the outer circuit and conduction current in the inner circuit [8].

3.2. Analysis of the Principle of Motion of BE-TENG Bionic Fins

In this paper, by designing a fin surface composed of a crankshaft-like structure with a bionic swing rod, the bionic electric eel's connected anal and caudal fins will realize a sinusoidal-like change of the fin surface through the action of ocean currents [9-10]. The bionic fin structure and the shape of the fin surface of the BE-TENG device are shown in Fig. 7(a). The length of the bionic fin structure of this device is $L=230$ mm, the width is $W=60$ mm, the bionic fin fluctuation direction is selected as x-axis, and the bionic fin swing rod swing direction is z-axis, and the coordinate system is established as shown in Fig. 7(b).



(a) Bionic fin (b) Bionic fin surface shape

Fig 7. Schematic diagram of bionic fin structure

The equation for the oscillation of the fin surface of a bionic fish with the ocean current is:

$$\left\{ \begin{array}{l} x(l, s, t) = l \\ y(l, s, t) = s \cos \alpha \\ \quad = s \cos \left\{ \alpha_{\max} \sin \left[2\pi \left(ft - \frac{1}{\lambda} \right) \right] \right\} \\ z(l, s, t) = s \sin \alpha \\ \quad = s \sin \left\{ \alpha_{\max} \sin \left[2\pi \left(ft - \frac{1}{\lambda} \right) \right] \right\} \end{array} \right. \tag{10}$$

In this equation: l is the change amount of the bionic fin along the direction of the current baseline (x -axis), s is the change amount along the direction of the swinging rod, t is the working time, α is the angle between the bionic swinging rod and the vertical direction, f is the swinging frequency of the bionic swinging rod, and λ is the wavelength of the traveling wave generated by the bionic fin; α_{\max} is the maximum angle between the bionic swinging rod swinging to one side and the vertical direction[11].

The angle of the i th bionic oscillating rod at the moment t is:

$$\alpha_i(l_i, t) = \alpha_{\max} \sin \left[2\pi \left(ft - \frac{l_i}{\lambda} \right) \right] \quad i = 1, 2, 3, \dots, 20 \quad (11)$$

In this equation: α is the angle between the i th bionic oscillating rod and the vertical direction at time t , and l_i is the amount of change of the i th bionic oscillating rod along the bionic fin in the direction of the current baseline (x -axis).

In order to study the nature of the bionic fins to remain smooth in the water, it is necessary to calculate the force generated during the swinging of multiple bionic swing rods, mainly considering the bionic fins due to the action of the current fluctuations generated by the action of the force (x -axis direction) as well as the lateral force (z -axis direction), the swing rods and the device's own gravity and buoyancy for the equilibrium force (y -axis direction), so ignored. The calculation equation of the force F_f and lateral force F_h after the bionic fin fluctuation is as follows:

$$F_f(t) = \int_S p(n_x dS) \quad (12)$$

$$F_h(t) = \int_S p(n_z dS) \quad (13)$$

In this equation: n_x is the projection of the unit normal vector \mathbf{n} of the bionic fin surface in the direction of the x -axis force, n_z is the projection of the unit normal vector \mathbf{n} of the bionic fin surface in the direction of the z -axis force, and S is the overall area of the fin surface of the multiple bionic fins.

The average force F_{fa} generated by the bionic fin movement and the lateral force F_{ha} are calculated as follows:

$$F_{fa} = \frac{1}{T} \int_T F_f(t) \cdot dt \quad (14)$$

$$F_{ha} = \frac{1}{T} \int_T F_h(t) \cdot dt \quad (15)$$

In this equation: T is the period of fin surface movement with the current.

In this paper, we do not discuss the direction of the force generated by the fin surface of the modal fish under the influence of ocean currents, and the instantaneous transverse force is approximately distributed symmetrically along the zero scale line, for which the average value is approximately zero, so we take the average value of the positive part of it for discussion[12]. Through the calculation study, it is found that the force generated by the bionic fin surface always alternates along the x -axis direction, and the direction of the transverse force alternates positively and negatively along the z -axis direction, from which it can be seen that the modal fin structure designed in this paper can effectively ensure that the BE-TENG device will not be overturned by the influence of ocean waves.

3.3. Comparative Output Performance Tests of Spiral Generation Structures

A single internal spiral power generator device of BE-TENG is taken, and an aluminum electrode material with a width of 60 mm is pasted on the upper layer of each layer of the spiral power generator device, and a PTFE dielectric layer material with a width of 60 mm is pasted on the

lower layer, and a single-layer PTFE-Al circular friction pair with an inner diameter of 40 mm and a ring width of 30 mm is used for the comparison of the output performance of the two devices. The two were placed in a speed-modulated multi-purpose oscillator, adjust the frequency to 1.0 Hz, simulating the BE-TENG vertical contact-separation mode of operation, wire connection multimeter to measure the output performance of the two open-circuit voltage UOC, short-circuit current ISC, measurement of the average value of the results of the 50 times as shown in Fig 8. . From the figure, it can be seen that the short-circuit current of the spiral structure power generation device increases significantly compared with the ordinary PTFE-Al friction pair, from 1.37 μA to 3.05 μA , an improvement of 2.23 times; the open-circuit voltage does not have a significant change, and it can be concluded that the spiral power generation structure has a certain enhancement for the performance of BE-TENG.

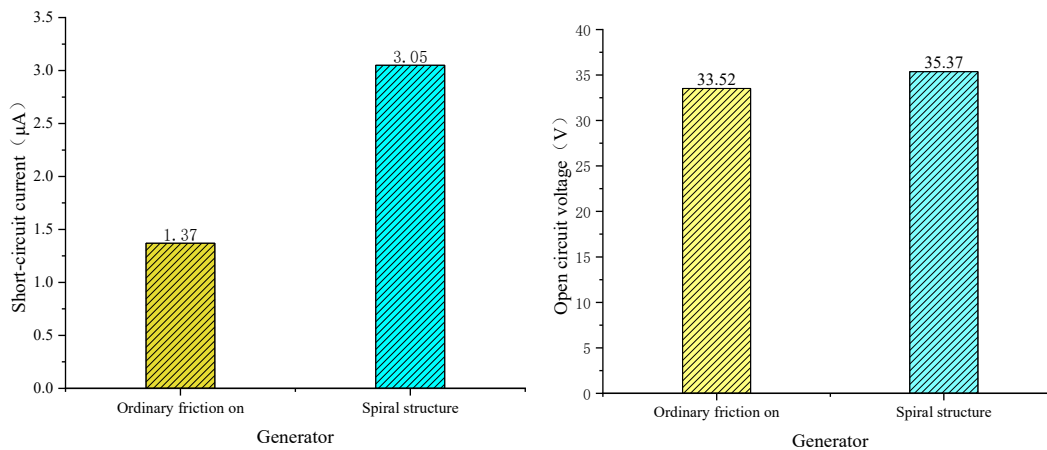


Fig 8. Comparison of output performance between normal friction pair and helical generation structure

3.4. Effect of Effective Friction Area on BE-TENG Output Performance

From equation (8), it can be seen that the effective friction area between the composite dielectric layer and the electrode layer will have an impact on the output performance of the BE-TENG, due to the existence of two helical structure power generators in the BE-TENG device and the maximum size of the aluminum electrode and the dielectric layer material that can be affixed between each layer approximates to a circle with an inner diameter of 40 mm and a ring width of 40 mm, therefore, in order to ensure that the electrode layer of the BE-TENG and the composite dielectric layer smoothly contact friction, control the composite dielectric layer and the electrode layer material of the same size. Keeping the inner diameter of the ring unchanged, the aluminum electrode and the composite dielectric layer are cut into rings with ring widths of 20 mm, 25 mm, 30 mm, 35 mm, and 40 mm, and the effective contact areas are calculated to be $40 \pi \text{ cm}^2$, $52.48 \pi \text{ cm}^2$, $66 \pi \text{ cm}^2$, $80.48 \pi \text{ cm}^2$, and $96 \pi \text{ cm}^2$, respectively, so as to make the effective contact area as a one-factor variable, and then investigate the relationship between the output performance and effective contact area of the friction nano-generator and the friction performance and effective contact area of the nano-generator. generator output performance in relation to the effective contact area. In particular, the BE-TENG friction pair spacing was controlled to be 30 mm, and the linear motor was controlled to have a water wave frequency of 1.0 Hz and an amplitude of 50 mm.

As shown in Fig. 9, a partial output performance graph of the intercepted BE-TENG after the stable working state is shown, when the size of the composite dielectric layer and the electrode layer reaches the maximum value of $32\pi \text{ cm}^2$, the short-circuit current of the BE-TENG reaches the peak value, which is 7.5 μA , and the open-circuit voltage at this time is 68.9 V. From the figure, it can be seen that the short-circuit current of the BE-TENG increases with the effective contact area and the open-circuit voltage increases with the effective contact area. It can be

seen from the figure that the short-circuit current of BE-TENG increases with the increase of the effective contact area, and the open-circuit voltage does not change significantly with the increase of the effective contact area, and this result also verifies the accuracy of the theoretical analysis. Therefore, in this paper, the size of the composite dielectric layer and the electrode layer with an inner diameter of 40 mm and a ring width of 80 mm are selected for the next investigation.

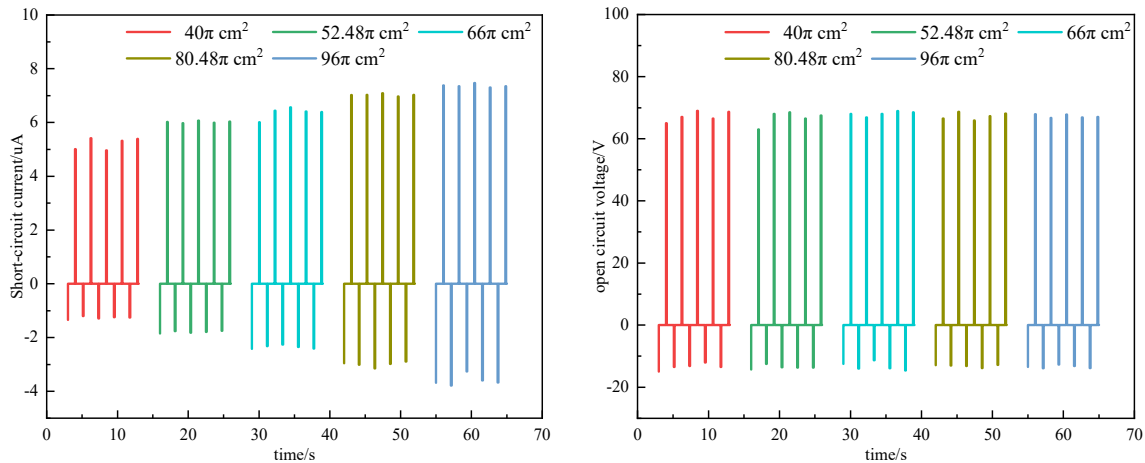


Fig 9. Effect of effective friction area between electrode layer and composite dielectric layer on BE-TENG output performance

3.5. Effect of Composite Dielectric Layer Thickness on BE-TENG Output Performance

Similarly, it can be seen from Eq. (8) that the thickness of the composite dielectric layer also affects the output performance of BE-TENG. On the basis of the previous section, composite dielectric layers with thicknesses of 0.1 mm, 0.2 mm, 0.3 mm, 0.4 mm, and 0.5 mm were fabricated by adjusting the size of the squeegee caliper on the heated flatbed coater, keeping other experimental factors unchanged, and choosing five composite dielectric layers with different thicknesses as one-factor variables to investigate the output performance of the friction nanogenerator in relation to the thickness of the composite dielectric layer. The relationship between the output performance of the friction nanogenerator and the thickness of the composite dielectric layer.

As can be seen in Fig. 10, the short-circuit current of BE-TENG increases with the thickness of the composite dielectric layer, and the open-circuit voltage does not change significantly. When the thickness of the composite dielectric layer is 0.5 mm, the short-circuit current of BE-TENG reaches the peak value, and the peak value of the short-circuit current is $10.38 \mu\text{A}$, and the open-circuit voltage is 70.2 V. It is worth noting that, when the thickness of the composite dielectric layer is 0.3 mm, the peak value of the short-circuit current is slightly larger than that of the composite layer with the thickness of 0.4 mm, which is probably due to the fact that in the process of fabricating composite dielectric layers with different thicknesses, the materials are not as thick as the composite dielectric layer. This may be due to the fact that in the process of making composite dielectric layers of different thicknesses, the time of material mixing and the temperature of the PTFE dielectric layer coating are different, leading to differences in the microstructure of the prepared composite dielectric layer, so that the surface contact area increases and the friction is more adequate. Since the output performance of BE-TENGs fabricated with 0.4 mm and 0.5 mm composite dielectric layers is not significantly improved compared with that of 0.3 mm composite dielectric layers, a composite dielectric layer with a thickness of 0.3 mm is chosen to further investigate the BE-TENG performance in order to save the cost of the experiment.

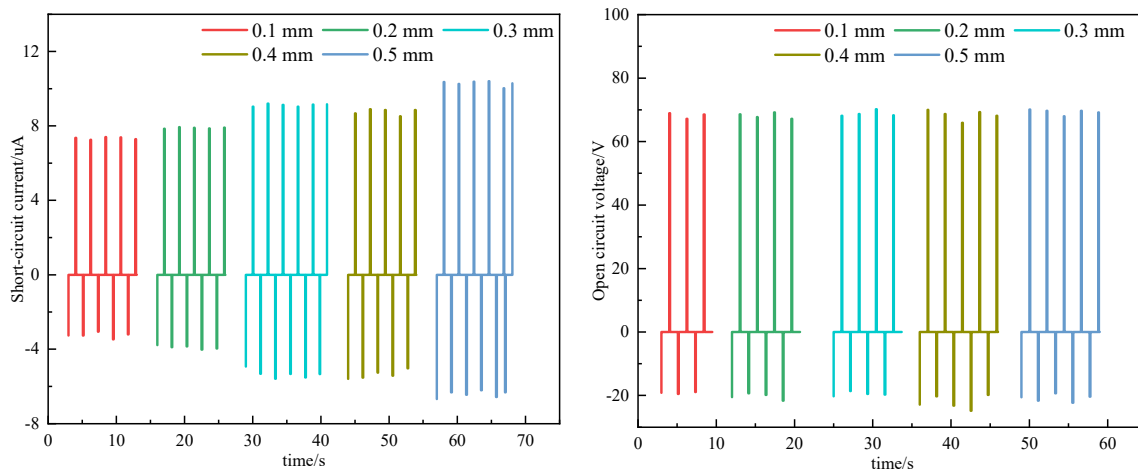


Fig 10. Effect of thickness of composite dielectric layer on the output performance of BE-TENG

4. Conclusion

In summary, based on vertical contact-separation friction nanogenerator, this paper designs a spiral power generation structure bionic electric eel-type friction nanogenerator based on the biological structure and power generation principle of electric eel. Firstly, this paper designs a BE-TENG structure with a semi-cylindrical shell as the main body, and combines the crankshaft-like structure and the biomimetic fin swing rod to simulate the electric eel's tail fin to ensure the balance of the device; secondly, this paper proposes a helical power generation structure, and the short-circuit current grows from $1.37 \mu\text{A}$ to $3.05 \mu\text{A}$ compared with the ordinary PTFE-Al friction pair under the same conditions, which is a 2.23-fold enhancement; and thirdly, it explores the relationship between the BE-TENG dielectric layer and the electrodes and the friction nanogenerator. potential relationship between BE-TENG dielectric layer and electrode layer, based on the theoretical foundation of vertical contact-separation friction nanogenerator, to explore the factors affecting the output performance of BE-TENG, and to study the influence of effective friction area between the composite dielectric layer and the electrode layer, the thickness of the composite dielectric layer, and the output performance of BE-TENG by controlling the variables of a single factor; finally, under the conditions of this experiment Finally, under this experimental condition, the best output performance of BE-TENG is obtained when the effective contact area between the composite dielectric layer and the electrode layer of BE-TENG is $32\pi \text{ cm}^2$ and the thickness of the composite dielectric layer is 0.3 mm. The optimized BE-TENG further improves its ability to collect blue energy, which is expected to provide new ideas for the application of the friction nanogenerator and the protection of the blue ocean environment.

References

- [1] Vanessa P. Perceived environmental threats, place attachment, and natural resource employment: predicting willingness to move from a threatened coastline. *Environmental Sociology*, 2023, 9(3): P313-326.
- [2] Abbas S M, Alhassany H D S, Vera D, et al. Review of enhancement for ocean thermal energy conversion system. *Journal of Ocean Engineering and Science*, 2023, 8(5): P533-545.
- [3] Khojasteh D, Shamsipour A, Huang L, et al. A large-scale review of wave and tidal energy research over the last 20 years. *Ocean Engineering*, 2023, P282
- [4] Sardana D, Kumar P. Influence of climate variability modes over wind-sea and swell generated wave energy. *Ocean Engineering*, 2024, P291: 116471.

-
- [5] He F, Liu Y, Pan J, et al. Advanced ocean wave energy harvesting: current progress and future trends. *Journal of Zhejiang University-SCIENCE A*, 2023, 24(2): P91-108.
- [6] Fan F R, Tian Z Q, Wang Z L. Flexible triboelectric generator. *Nano energy*, 2012, 1(2): P328-334.
- [7] Zhang X, Hu J, Yang Q, et al. Harvesting multidirectional breeze energy and self-powered intelligent fire detection systems based on triboelectric nanogenerator and fluid-dynamic modeling. *Advanced Functional Materials*, 2021, 31(50): 2106527.
- [8] He W, Shan C, Wu H, et al. Capturing dissipation charge in charge space accumulation area for enhancing output performance of sliding triboelectric nanogenerator. *Advanced Energy Materials*, 2022, 12(31): 2201454.
- [9] Hwang H J, Choi D. The coupled effects of an electron blocking layer beneath tribomaterials for boosted triboelectric nanogenerators. *Functional Composites and Structures*, 2021, 3(2): 025004.
- [10] Wang X, Niu S, Yin Y, et al. Triboelectric nanogenerator based on fully enclosed rolling spherical structure for harvesting low-frequency water wave energy. *Advanced Energy Materials*, 2015, 5(24): 1501467.
- [11] Qu Z, Huang M, Chen C, et al. Spherical triboelectric nanogenerator based on eccentric structure for omnidirectional low frequency water wave energy harvesting. *Advanced Functional Materials*, 2022, 32(29): 2202048.
- [12] Ronaldo A, Flaminio S, Andrews S, et al. Polydimethylsiloxane Composites Characterization and Its Applications: A Review. *Polymers*, 2021, 13(23): P4258-4258.